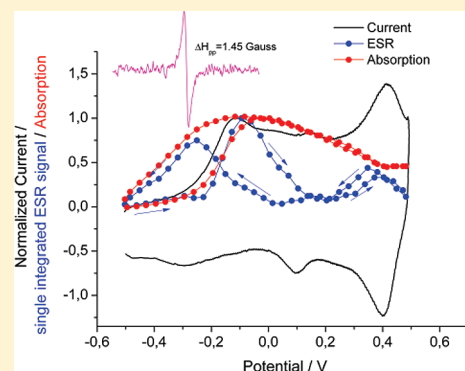


# How Linear Is “Linear” Polyaniline?

Evgenia Dmitrieva and Lothar Dunsch\*

Center of Spectroelectrochemistry, Department of Electrochemistry and Conducting Polymers,  
Leibniz Institute of Solid State and Materials Research, Helmholtzstrasse 20, D-01069 Dresden, Germany

**ABSTRACT:** The structure of emeraldine salt and emeraldine bases with different molar weight and their behavior in electrochemical doping was studied by different spectroscopic and spectroelectrochemical techniques. By Fourier transform infrared (FTIR) spectroscopy, the branching of the polymer chain at tri- and tetrasubstituted benzene rings as well as the presence of small amounts of phenazine units are shown. The branching of the polymer chains increases with the increasing of the molar weight of emeraldines. The optical transitions in protonated and unprotonated emeraldine were studied by ultraviolet–visible near-infrared (UV–vis NIR) spectroscopy. By comparison of the electron spin resonance (ESR) spectra of emeraldine in protic solvents and acidic solutions, the emeraldine bases are shown to be to some extent protonated. Applying in situ ESR–UV–vis NIR spectroelectrochemistry, the charged states in emeraldines upon p-doping were investigated considering the influence of the nonideal “linear” polymer structures. The initial stage of oxidation of the emeraldine base and salt consists of the different charged states. The phenazine units in the polymer chains stabilize the charged states in the emeraldines upon p-doping.



## INTRODUCTION

The chemical structure of polyaniline (PANI) is often given as a linear model with a tetrameric repeating unit (Figure 1). In the most reduced state of polyaniline (leucoemeraldine), all nitrogen atoms in the repeating unit are of amine type, and all rings are benzenoid. In the fully oxidized state (pernigraniline), all nitrogen atoms are of imine type, and the benzenoid rings alternate with quinoid ones. In the semioxidized form (emeraldine), one-half of nitrogen atoms are of imine type, whereas the remaining one-half are of amine type. The repeat unit contains three benzenoid rings per one quinoid ring.

On the basis of the linear PANI structures, the well-accepted polaron–bipolaron model for conducting polymers is interpreted as follows: the polaron (radical cation) is the singly oxidized form of a polymer segment with spin  $s = 1/2$  and two optical transitions; the bipolaron (dication) is a doubly oxidized form, which is diamagnetic and has one optical transition.<sup>1,2</sup> It was shown earlier by in situ ESR–UV–vis spectroelectrochemistry that the polaron structure in PANI is formed by symproportionation reaction of the bipolaron and the neighboring neutral polymer segments.<sup>3</sup> However, other charged species formed during p-doping of conducting polymers are also reported. Brédas et al. suggested a new charged state of “two polarons on a single chain” for long oligothiophenes, which is energetically favored and has two bands in the absorption spectra.<sup>4</sup> We have shown earlier that the most important intermediate formed during aniline polymerization, the *p*-aminodiphenylamine, forms a  $\pi$ -dimer of two radical cations under oxidation in acidified organic solvents.<sup>5</sup> The  $\pi$ -dimer is characterized by two optical transitions, which are blue-shifted with respect to the two bands of the corresponding radical cation.<sup>6,7</sup>

More recently, the equilibrium and kinetics of conjugated systems with either polarons and bipolarons or polarons and polaron pairs ( $\pi$ -dimers) as charged states were compared by Paasch et al.<sup>8</sup>

It is well accepted in the scientific community that PANI consists of a linear arrangement of the monomer.<sup>9</sup> While most studies on the electronic structure of polyaniline and its change upon doping use the linear structure model for a structural explanation of the charged states, the influence of phenazine structures on the formation of charged states in polyaniline is not yet studied and understood in detail. It was earlier shown for chemically and electrochemically prepared PANI that phenazine rings have to be considered as a part of the polymer chain.<sup>10–12</sup> By comparison of IR spectra of electrochemically prepared PANI and aniline–phenosafranin copolymers, it was shown in our previous work that polyaniline consists also of phenazine-like units.<sup>13</sup> Several IR vibrations were ascribed to such phenazine-like units and also to 1,2,4-trisubstituted benzene nuclei in the phenazine skeleton in PANI. The presence of substituted phenazine units, formed by the intramolecular cyclization of branched PANI chains, has been identified by the appearance of characteristic FTIR bands at 1623, 1414, 1208, 1144, 1136, 1108  $\text{cm}^{-1}$  and Raman bands at 1645–1630, 1420–1400, 1380–1365,  $\sim 575$ , and  $\sim 415 \text{ cm}^{-1}$ .<sup>14–16</sup> Do Nascimento et al. demonstrated that the cross-linking units in PANI nanofibers are phenazine- and/or oxazine-like structures, which show Raman bands at ca. 1640, 1380, and 578  $\text{cm}^{-1}$ .<sup>17–19</sup> Genies et al.

Received: January 20, 2011

Revised: April 20, 2011

Published: May 03, 2011

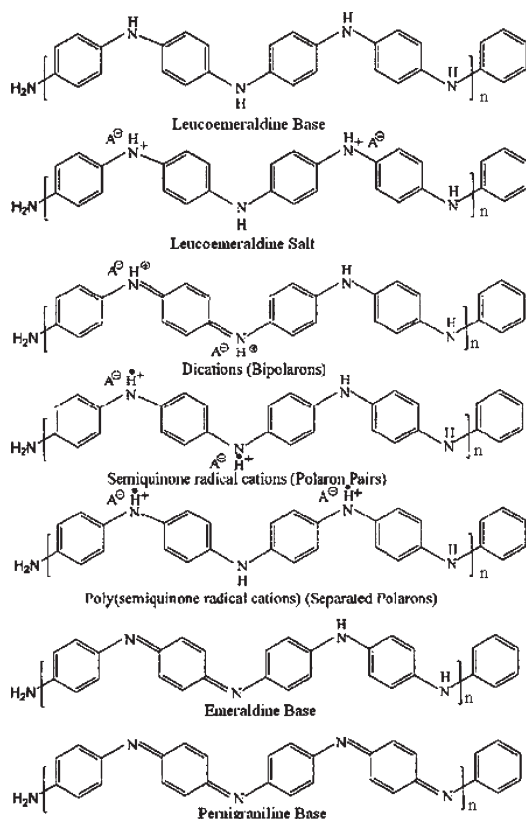


Figure 1. Structure of linear PANI and its different oxidation states.

suggested that the so-called middle peak in the cyclovoltammogram of PANI is attributed to the presence of the phenazine rings, because the intensity of the peak increases upon copolymerization of aniline with phenazine and by oxidation of aniline at a higher potential than the second voltammetric peak.<sup>20</sup> Our previous studies of PANI and aniline–phenosafranin copolymers showed that the middle peak in the cyclovoltammograms of PANI is attributed to the benzo/hydroquinone couple in the polymer structure, which is formed by the hydrolysis of imine groups.<sup>21</sup>

As the linear form of PANI prepared chemically is often applied in studies of charge transfer reactions, it is to be clarified whether only linear chains are existent in such structures of so-called “linear” PANI and whether their real structure has any influence on the stabilization of charged states in such kind of polymer. The PANI structures have different weight average molecular weights, which are to be considered in the presentation even if it is not explicitly given.

## EXPERIMENTAL SECTION

Commercially available emeraldine base with different weight average molecular weight (average  $M_w \approx 5000$ , 50 000, and 300 000, Aldrich) and emeraldine salt (average  $M_w > 15\,000$ , Aldrich) are denoted as EB1, EB2, EB3, and ES, respectively. Dimethyl sulfoxide (DMSO, puriss., Aldrich) and *m*-cresol (99%, Aldrich) were used as solvent. The FTIR spectra of emeraldine were measured on KBr pellets at room temperature in transmission mode by an IFS 66v spectrometer (Bruker Optics, Germany). For each spectrum, 250 interferograms with a resolution of  $2\text{ cm}^{-1}$  were sampled. The UV–vis NIR spectroscopic

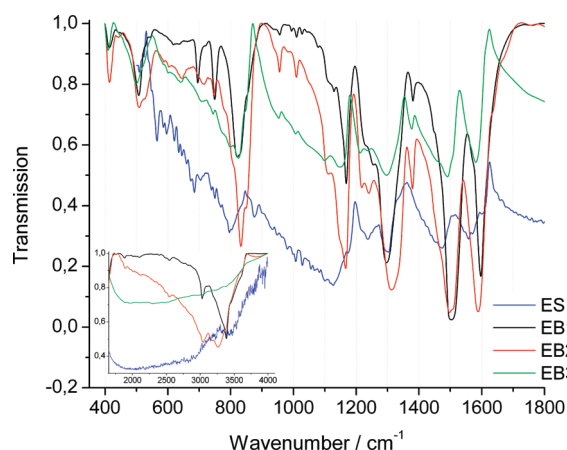


Figure 2. FTIR spectra of the emeraldine base of different molecular weights and of the emeraldine salt. Inset: FTIR spectra in the range  $1700\text{--}4000\text{ cm}^{-1}$ .

measurements were carried out in a quartz cell (light path 10 mm, Hellma Analytics, Germany) with an MPC-3100 spectrometer (Shimadzu, Japan).

The ESR–UV–vis NIR spectroelectrochemical technique was described earlier.<sup>3</sup> For ESR measurements, an EMX X-band spectrometer (Bruker BioSpin, Germany) at 100 kHz modulation and a microwave power of 2 mW was used. The ESR spectra were recorded in a standard optical cavity 4104OR (Bruker BioSpin, Germany) allowing the connection of two optical wave guides to measure in situ the electronic absorption spectra in transmission simultaneously with the ESR spectra. For UV–vis NIR spectroscopy, two fiber optic spectrometers (Avantes, The Netherlands) applying the AvaSoft 7.5 software were used. The spectrometers AvaSpec-2048x14-USB2 with the CCD detector and AvaSpec-NIR256-2.2 with the InGaAs detector were used. A balanced deuterium–halogen lamp AvaLight-DH-S-BAL serves as the light source. The in situ ESR–UV–vis NIR spectroelectrochemical measurements were controlled by a PG 285 potentiostat (HEKA Electronic, Lambrecht, Germany) equipped with the PotMaster v2x40 software and triggering both the ESR spectrometer and the UV–vis NIR spectrometer modules. The spectroelectrochemical quartz flat cell was equipped with a working electrode as a laminated ITO electrode (thickness of 0.3 mm, specific surface conductivity of  $20\text{ }\Omega/\square$ , Merck) with an area of  $0.096\text{ cm}^2$ . A rectangular black mask with a hole smaller than the active electrode surface of the laminated ITO electrode was fixed on the flat cell. The counter electrode consists of the platinum wire. A silver chloride-coated silver wire with a thin flexible Teflon tube served as the pseudo-reference electrode (all potentials here are given vs silver pseudo-reference electrode). The spectroelectrochemical measurements were carried out under nitrogen atmosphere and at room temperature. The polymers were dissolved in DMSO, deposited on an ITO electrode by drop coating, followed by solvent evaporation. The solubility of the polymers in DMSO decreases with increasing molar weight. The spectroelectrochemical investigations of the polymers were carried out in aqueous solution of 0.1 M sulfuric acid (Merck, 95–97%) and 0.01 M sodium *p*-toluenesulfonate (Merck, 98%) because of their insolubility in water.

For ESR measurements, an EMX plus X-band spectrometer (Bruker BioSpin, Germany) at 100 kHz modulation and an EMX plus standard cavity 4119HS (Bruker BioSpin, Germany) were

**Table 1.** Main FTIR Bands of EB1, EB2, EB3, and ES in the Frequency Range 4000–400 cm<sup>−1</sup> and Their Assignments<sup>a</sup>

EB1	EB2	EB3	ES	assignment
3480sh			3554s	$\nu(\text{N-H})$ in Ar-NH <sub>2</sub>
3388s	3388sh	3370s		$\nu(\text{N-H})$ H-bonded or $\nu(\text{=NH}^+)$ H-bonded
3216sh	3278s			$\nu(\text{N-H})$ in Ar-NH <sub>2</sub> , or $\nu(\text{N-H})$ in Ar-NH-Ar
3026s	3040s	3012s		$\nu(\text{C-H})$ , $\nu(\text{N-H})$ H-bonded
	1632sh			$\nu(\text{C=N})$ , $\nu(\text{C=C})$
1597s	1589s	1581s		$\nu(\text{C=C})$ in N=Q=N
1573sh <sup>1</sup>	1565sh <sup>1</sup>	1561sh <sup>1</sup>	1556s <sup>2</sup>	<sup>1</sup> $\nu(\text{C=C})$
				<sup>2</sup> $\nu(\text{C=C})$ in ES (red shift of the band at 1597 cm <sup>−1</sup> )
1504s,br	1507s	1506sh		$\nu(\text{C=C})$ in N-B-N
	1496s	1491s		
1468sh,vw <sup>1</sup>	1469sh,w <sup>1</sup>	1460sh,m <sup>1</sup>	1470s <sup>2</sup>	<sup>1</sup> $\nu(\text{C=N})$ and $\nu(\text{C=C})$ in Phz
				<sup>2</sup> $\nu(\text{C=C})$ in ES (red shift of the band at 1505 cm <sup>−1</sup> )
1449sh,w	1449sh	1454sh		$\nu(\text{C=C})$
1418sh,vw	1415sh,vw	1413sh,vw		$\nu(\text{C=C})$ in Phz
1380m	1379m	1376m		$\nu(\text{C-N})$ in the neighborhood of a quinoid ring (in QB <sub>t</sub> Q)
1333sh	1333sh	1328sh	1337w	$\nu(\text{C-N})$ in quinoid imine units
1297s	1312s	1296s	1300s	$\nu(\text{C-N})$ in secondary aromatic amines (in QB <sub>c</sub> Q, QBB, BBQ) or N-H bending
1254m <sup>1</sup>	1240m <sup>1</sup>	1236m <sup>1,2</sup>	1237s <sup>2</sup>	<sup>1</sup> $\nu(\text{C-N})$ in secondary aromatic amines (in BBB)
1231m <sup>1</sup>				<sup>2</sup> $\nu(\text{C-N}^+)$ in polaron lattice
1216sh,vw	1217m	1213m	1218sh	$\nu(\text{C-N})$ in primary and secondary aromatic amines or $\delta(\text{C-H})$ in 1,4 disubst ring or in Phz
1168s	1166s	1164sh	1170sh	$\delta(\text{C-H})$ a mode of N=Q=N
1156sh <sup>1</sup>	1147sh <sup>1</sup>	1144m <sup>1</sup>	1124m <sup>2</sup>	<sup>1</sup> $\delta(\text{C-H})$ a mode of Q=N <sup>+</sup> H-B or B-NH-B
				<sup>2</sup> $\delta(\text{C-H})$ a mode of Q=N <sup>+</sup> H-B or B-NH-B in ES (red shift of the band at 1166 cm <sup>−1</sup> )
1111m	1113m	1099m		$\delta(\text{C-H})$ in 1,4 disubst or 1,2,4 trisubst ring
1077w				$\delta(\text{C-H})$ in monosubst ring
1027vw				
1010w	1008w	1007w		$\delta(\text{C-H})$ in 1,4 disubst or in monosubst ring
956vw	956w	953w		ring def vib or $\delta(\text{C-H})$ in Phz
882sh,vw	881sh,vw			$\gamma(\text{C-H})$ in 1,2,4-trisubst ring (1H) or in 2-subst Phz
		876sh	877w	$\gamma(\text{C-H})$ in 1,2,4 trisubst ring (2H) or 1,2,4,5 tetrasubst ring or in 2- and 2,3-subst Phz
854sh	848sh	847sh		$\gamma(\text{C-H})$ in 1,2,4 trisubst or 1,2,4,5 tetrasubst ring or in 2- and 2,3-subst Phz
820s, 830s	832s	826s		$\gamma(\text{C-H})$ in 1,4 disubst or skeletal vib in Phz
804sh,vw	808sh <sup>1</sup>	799sh <sup>1, 2</sup>	803s <sup>2</sup>	<sup>1</sup> $\gamma(\text{C-H})$ in 1,4 disubst ring
				<sup>2</sup> $\gamma(\text{C-H})$ in ES (red shift of the band at 820 cm <sup>−1</sup> ) in 1,4 disubst ring or NH <sub>2</sub> <sup>+</sup> rocking
	782sh	776sh		$\gamma(\text{C-H})$ in 1,2 disubst, 1,2,4 trisubst, or 1,2,4,5 tetrasubst ring or in 2- and 2,3-subst Phz
749m	746w	744w	750w	$\gamma(\text{C-H})$ in monosubst ring, in 1,2-disubst ring, or in Phz
715sh	716w	710w		$\gamma(\text{C-H})$ in 1,2-disubst ring
695m	695sh	695sh,w	685w	out-of-plane ring def vib in monosubst ring
646w	645w	630w		in-plane ring def vib in 1,4-disubst ring
	525sh	522sh		in-plane ring def vib in 1,2-disubst ring
	603w	600w		skeletal vib in Phz
507m	509m	499m	504m	out-of-plane ring def vib in 1,4-disubst or in monosubst ring
414m	413m	410m	410m	out-of-plane ring def vib

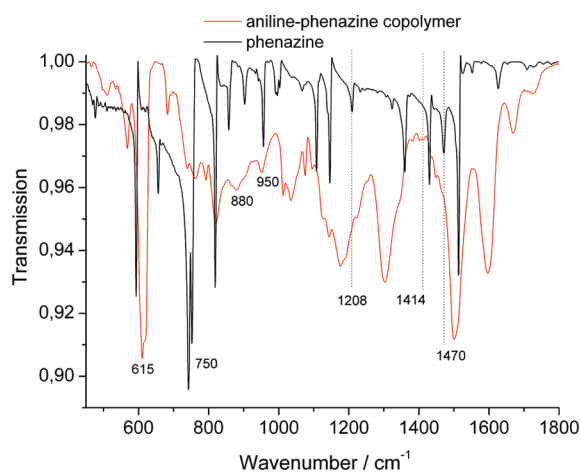
<sup>a</sup>  $\nu$ , stretching;  $\delta$ , in-plane bending;  $\gamma$ , out-of-plane bending; s, strong; m, medium; w, weak; vw, very weak; sh, shoulder; b, broad; B, benzene ring; Q, quinoid ring; Phz, phenazine; vib, vibration. Assignments are based on refs 21–36.

used. The ESR spectra were measured at atmospheric conditions. For the spin number determination, a microwave power of 0.02 mW was used to avoid the sample saturation. The spin concentrations in 10 mg of each powder were determined by doubly integrating the ESR signal and calculation in spins per gram. The ESR spectra of the polymer powders measured in a vacuum (at  $1 \times 10^{-4}$  mbar) show that oxygen presence has no influence on the line widths of the ESR signal and spin number in the polymer.

## RESULTS AND DISCUSSION

**FTIR Spectroscopy.** The IR spectroscopic results with the main infrared bands of emeraldines as a powder and their assignments are shown both in Figure 2 and in Table 1.

The wavenumber range 1200–600 cm<sup>−1</sup> comprises the in-plane and out-of-plane bending of C–H bands on aromatic rings. The band intensities and positions in this region depend on the substitution pattern in the aromatic ring. The bands at 880, 876,



**Figure 3.** FTIR spectra of the phenazine polymer and the aniline-phenazine copolymer.

850, and 780  $\text{cm}^{-1}$  present the branching polymer chains with tri- and tetra-substituted aromatic rings in emeraldines. However, the 1,2,4-tri- or 1,2,4,5-tetrasubstituted benzene rings can also be associated with the 2- or 2,3-substituted phenazine units in the polymer structure, respectively.<sup>27</sup> The band at ca. 820  $\text{cm}^{-1}$  corresponds to the C–H bending in 1,4-disubstituted benzene rings as well as to skeletal vibrations in the phenazine ring. The intensity of the IR peaks attributed to the branching structure and the phenazine units become more intensive in the row EB1–EB2–EB3. Therefore, the branching of the polymer structure increases with increasing molecular weight of emeraldines. The peaks attributed to the phenazine units in the polymer are marked in *italics* in Table 1.

For comparison with emeraldines, aniline-phenazine copolymer was electrochemically prepared. The spectrum of a copolymer has a band at 1470  $\text{cm}^{-1}$ , which is also present in the spectrum of phenazine (Figure 3). This band corresponds to the ring stretching mode of phenazine units.<sup>37</sup> The peak at 1415  $\text{cm}^{-1}$  was associated by Trchova et al. with phenazine-like units in the structure of polyaniline.<sup>15</sup> The spectrum of phenazine has a strong skeletal and a C–H in-plane deformation band in the region at 1215–1200 and 959–955  $\text{cm}^{-1}$ , both of which are visible in the spectra of all polymers. The spectrum of the aniline-phenazine copolymer presents the intensive double band at around 615  $\text{cm}^{-1}$  close to the peak at 592  $\text{cm}^{-1}$  in the spectrum of phenazine. However, phenazine and substituted derivatives show a strong band (often double band) at ca. 750  $\text{cm}^{-1}$  due to out-of-plane deformation vibrations of the phenazine ring.<sup>27</sup> The pronounced peak at 880  $\text{cm}^{-1}$  is attributed to the 2-substituted phenazine ring. These bands are observed in spectra of all polymers and confirm the presence of phenazine units in their structure.

The IR peaks of the polymers in the wavenumber range 3500–1200  $\text{cm}^{-1}$  are consistent with the peaks reported earlier for polyaniline (Table 1). In comparison to EB, ES gives a broad band at 1800–3000  $\text{cm}^{-1}$  that is typical for conducting form of PANI and attributed to  $\pi$ -electron delocalization in the polaron structure of ES.<sup>38</sup> The spectrum of EB3 shows the same band but with lower intensity than ES. The narrow bands at ca. 1590 and 1500  $\text{cm}^{-1}$  correspond to N=Q=N and N–B–N stretching in polyaniline. The bands have an obvious red-shift by protonation in ES to 1556 and 1470  $\text{cm}^{-1}$ , respectively. The larger intensity at

1504  $\text{cm}^{-1}$  for EB1 indicates that the benzene rings dominate the polymer chains. The peak at 1166  $\text{cm}^{-1}$  in EB is attributed to  $\delta(\text{C–H})$  in N=Q=N and typical for EB. This peak is shifted to 1124  $\text{cm}^{-1}$  in ES and can be assigned to the protonated doped chains of PANI and was commonly observed in the spectra of EB protonated with strong acids.<sup>39</sup> The band at ca. 830  $\text{cm}^{-1}$  that corresponds to  $\gamma(\text{C–H})$  in 1,4-disubstituted benzene ring in ES is red-shifted to 803  $\text{cm}^{-1}$ . The red shift of the IR absorption peaks is connected with the conversion of the quinoid rings to the benzene rings by protonation and indicates the increasing degree of charge delocalization on the polyaniline backbone due to protonation.<sup>40</sup> All IR bands in the spectrum of EB3 are slightly shifted to lower frequencies. The red shift together with the broad band in the region 1800–3000  $\text{cm}^{-1}$  indicates that the nitrogen atoms are protonated in the emeraldine base with high molecular weight. The band at 1380  $\text{cm}^{-1}$  is attributed to C–N stretching in the neighborhood of a quinoid ring and is typical for EB. In the spectrum of ES, this peak is absent. The band at 1237  $\text{cm}^{-1}$  is associated with C–N stretching in secondary aromatic amines. In the spectrum of ES, this band is strongly visible and attributed to C–N<sup>++</sup> stretching in a polaron lattice. The bands at 1556, 1337, and 1170  $\text{cm}^{-1}$  indicate that quinoid rings are present in ES.

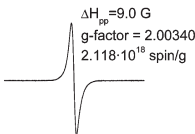
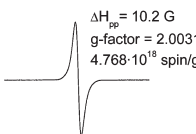
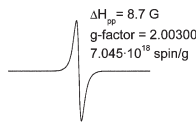
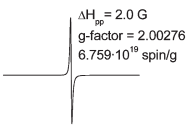


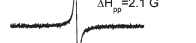
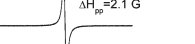
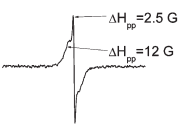
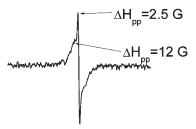
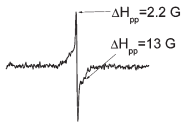
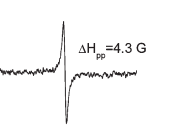

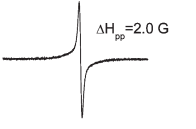
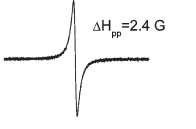
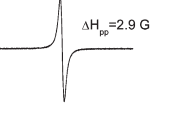
It was already shown by FTIR spectroscopy that emeraldines have branches in their polymer chains and contain small amounts of phenazine units in their structures. The bands at 1470, 1414, 950, 830, and 600  $\text{cm}^{-1}$  are attributed to the phenazine rings in PANI. The bands at 880, 876, 850, and 780  $\text{cm}^{-1}$  present the branching polymer chains and can be associated with the 2- or 2,3-substituted phenazine units in the polymer structure. The branching of the polymer structure increases with increasing molecular weight of emeraldines. The branching of the polymer chain and the existence of phenazine units have to be considered for the explanation of the stabilization of charged states in “linear” PANI. Therefore, both the EB and the ES structures do not have an ideal linear structure.

**UV–Vis NIR and ESR Spectroscopy.** All polymers show ESR signal in the powder form (Table 2). The ESR signal gives a line width ( $\Delta H_{\text{pp}}$ ) of around 9–10 G for emeraldine bases and 2 G for ES, respectively. The narrow ESR signal in ES is due to the delocalization of polarons in the polymer chain. A minor decrease of the  $g$ -factor values in the row EB1–EB2–EB3–ES is observed. The  $g$ -factor of 2.00276 in ES is close to the  $g$ -factor value of the free electron. ES shows a spin concentration of  $6.759 \times 10^{19}$  spin/g. The number of monomer units per spin was calculated for the linear polyaniline structure to be 1 spin per 100 aniline units in the emeraldine salt. In general, the spin concentration of emeraldine bases increases with increasing molecular weight of the polymers. The maximal value of the spin concentration in emeraldine bases is observed for EB3, which is in good agreement with the broad IR band in the region 1800–3000  $\text{cm}^{-1}$  attributed to the conducting form of PANI.

The UV–vis spectra of EB and ES in aprotic solvent (DMSO) (Figure 4a) show two absorption bands at 331 and 626 nm. These bands are attributed to the  $\pi$ – $\pi^*$ -transition of the benzene rings and the absorption of the quinoid rings, respectively.<sup>41</sup> The intensities of both bands in EB2 and EB3 are equal, while the intensity of the peak at 331 nm in EB1 is higher than that at 626 nm. It indicates that EB1 with lower molar mass has larger amounts of benzene rings than other emeraldine bases. It correlates with the major peak at 1504  $\text{cm}^{-1}$  attributed to C–C stretching in benzene rings in the IR spectra of EB1.



Table 2. ESR Signal of the Emeraldine Bases and Salt

	EB1	EB2	EB3	ES
Polymers as a powder				
Polymers dissolved in DMSO				
Polymers dissolved in <i>m</i> -cresol				
Polymers on an ITO electrode in electrolyte				

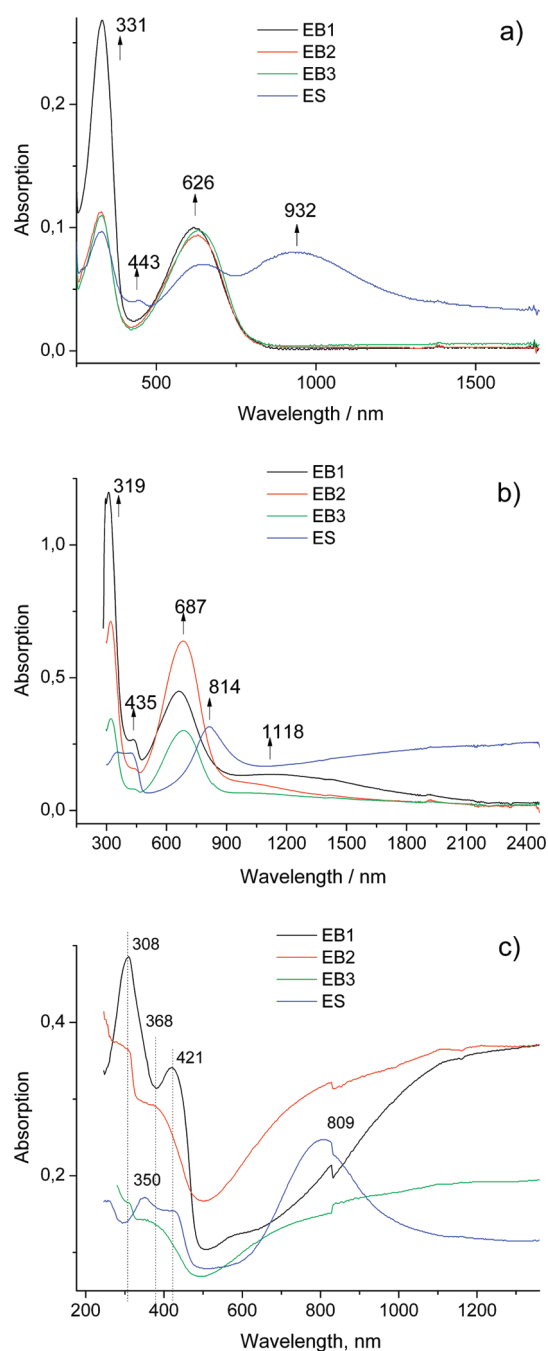
EB1 dissolved in DMSO gives no ESR signal, while EB2 has a weak broad ESR signal. Dramatic changes of the ESR signal are observed by dissolution of EB3 in this solvent. The line width decreases from 8.7 to 2.1 G, indicating the formation of a conducting form of PANI, while the UV–vis NIR spectra of EB3 in DMSO present no bands corresponding to a polaron structure in the polymer. This is caused by the fact that ESR spectroscopy is very sensitive for the detection of spins in the polymer.

The strong optical transition at 443 nm and the broad absorption at 932 nm in ES are characteristic for localized polarons (short conjugation length) and were assigned as the transitions from polaron band to  $\pi^*$ -band and from the  $\pi$ -band to the polaron band, respectively.<sup>42</sup> The presence of the band at 645 nm in ES indicates that quinoid segments are present in the polymer chains. It coincides with the presence of peaks at 1556, 1337, and 1170  $\text{cm}^{-1}$  attributed to the quinoid rings in the IR spectra of ES.

The absorption bands characteristic for ES are blue-shifted to 435 and 814 nm in *m*-cresol as protic solvent (Figure 4b). The spectrum of ES presents the “free-carrier tail” in the NIR region from 1200 nm. This broad band is together with the band at ca. 440 nm characteristic for the delocalized polaron structure (long conjugation length) according to ref 43. The ESR signal of ES has a  $\Delta H_{pp}$  value of 4 G (Table 2). The peak at 319 nm in EB is shifted to 356 nm in ES. There is no peak at 687 nm in the spectrum of ES in *m*-cresol as no quinoid rings in ES are present in protic solvent. The spectra of emeraldine bases in *m*-cresol have additional absorption bands at 435 and in the range of ca. 1000–1100 nm. The ESR spectra of all emeraldine bases show

two overlapping signals with  $\Delta H_{pp}$  values of 2.5 and ca. 10 G. The ESR signal with a line width of 2.5 G is caused by the delocalized polaron structure in emeraldine bases as a consequence of the partially protonation of the polymer. The ESR signal of the emeraldine bases with  $\Delta H_{pp}$  values of 10 G is close to that observed in the ESR spectra of the polymer as a powder. The signal with a  $\Delta H_{pp}$  value of 2.5 G disappears in the ESR spectra of emeraldine bases in *m*-cresol measured after 48 h (not shown in Table 2). Instead, an ESR signal with a broad line of ca. 9 G line width dominates the spectrum. Therefore, the ESR signal with  $\Delta H_{pp}$  value of 2.5 G is attributed to polarons stabilized on the linear polymer chains. In this case, the polaron is distributed over several monomer units in linear arrangement. The ESR signal of the line width of ca. 9 G can be associated with the localized polarons stabilized near the phenazine-like units. Therefore, a distribution of the charge in the delocalized and localized state along the polymer chains in the emeraldine bases is present in *m*-cresol solutions.

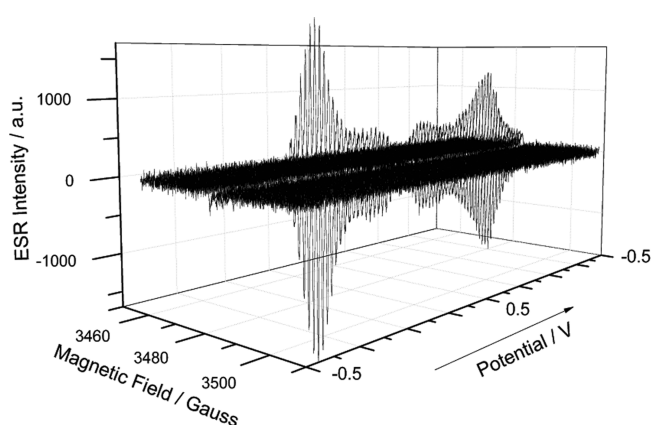
By using electrolyte solutions of pH 0.7, all polymers have a narrow ESR signal with a line width of 2–3 G. The ESR spectra of EB1 and EB2 measured in DMSO and in the electrolyte solution clearly demonstrate the existence of a protonated form of the emeraldine bases and the formation of the polaron structure in acidic solution. The absorption spectra of emeraldine bases have a single band at ca. 420 nm and a broad band in the NIR region that are absent in the spectra measured in DMSO solution (Figure 4c). The change of the optical bands of the emeraldine salt and base in electrolyte solution during their oxidation will be followed by *in situ* ESR–UV–vis NIR spectro-electrochemistry (see below).



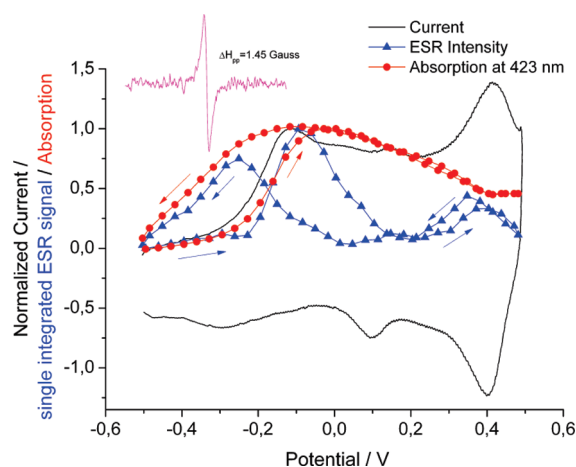
**Figure 4.** UV-vis NIR spectra of emeraldine bases and salt recorded in DMSO (a) and *m*-cresol (b) solution. (c) UV-vis NIR spectra of emeraldines in aqueous solution of 0.1 M sulfuric acid and 0.01 M sodium *p*-toluenesulfonate; the polymers were dissolved in DMSO and deposited on an ITO electrode by drop coating.

The optical transitions in protonated and unprotonated emeraldine forms were investigated by UV-vis NIR spectroscopy. By comparison of the ESR spectra of emeraldines in solutions of different acidity, it was shown that the polymers have a polaron structure in protic solvents and acidic solutions as a consequence of the protonation of the polymer chains.

**In Situ ESR-UV-Vis NIR Spectroelectrochemistry.** *Emeraldine Salt.* The ESR response of the emeraldine salt during its oxidation/rereduction (Figure 5) gives different states in the

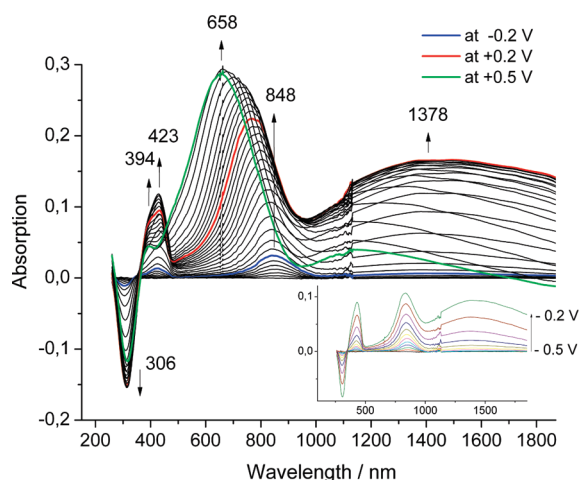


**Figure 5.** The ESR response of ES during the voltammetric scan in aqueous solutions of 0.1 M sulfuric acid and 0.01 M sodium *p*-toluenesulfonate.

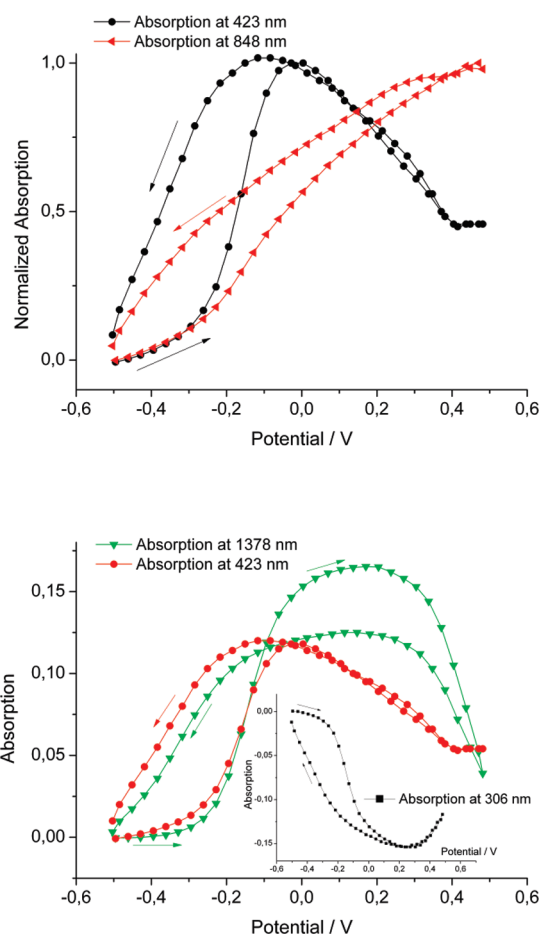


**Figure 6.** Potential dependence of current, single integrated ESR signal, and absorbance at 423 nm of ES recorded during the forward scan in aqueous solutions of 0.1 M sulfuric acid and 0.01 M sodium *p*-toluenesulfonate. All units are normalized with respect to the maximum values.

emeraldines. The emeraldine salt in its “uncharged state” has a narrow ESR signal with a  $\Delta H_{pp}$  value of 1.45 G. On the basis of the polaron–bipolaron model, the single-line ESR spectrum is attributed to delocalized polarons in the polymer chains. The potential dependence of the single integrated ESR signal has a first maximum at  $-0.09$  V, while the second maximum is of essentially lower intensity at  $0.4$  V (Figure 6). The large hysteresis of this potential dependence during the first redox peak is influenced by the conductivity. The ESR response at the first redox peak is broader in the back scan and has a lower intensity than that in the forward scan, which points to irreversible changes in the polymer at high potentials. The first maximum in the potential dependence of the single integrated ESR signal is associated with the polaron (of cation radical nature); the second maximum can be attributed to a polaron interaction with a bipolaron structure (like a trication radical) on the polymer chains. Genies et al. have proposed the structure  $-B-NH-B-NH^+-$  for the first one, involving conjugated aromatic aniline rings, and  $=Q-NH=Q-N^+=$  for the second one, involving conjugated quinoid rings.<sup>44</sup> The last structure is hardly probable.

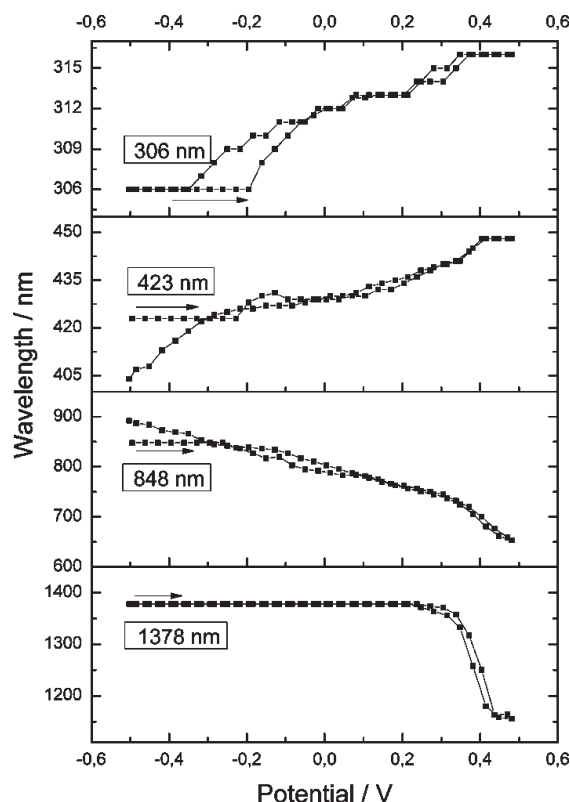


**Figure 7.** UV-vis NIR spectra of ES recorded in aqueous solution of 0.1 M sulfuric acid and 0.01 M sodium *p*-toluenesulfonate during the forward scan in the potential region from  $-0.5$  to  $+0.5$  V (scan rate  $3.3$  mV/s). Inset: UV-vis NIR spectra for the potential region from  $-0.5$  to  $-0.2$  V.



**Figure 8.** Potential dependence of the absorbance at different wavelengths during oxidation/reduction of ES.

Obviously, the cation radical is formed close to existing bipolarons. In other words, there is the trication radical formation on the polymer chains with several monomer units in linear arrangement.

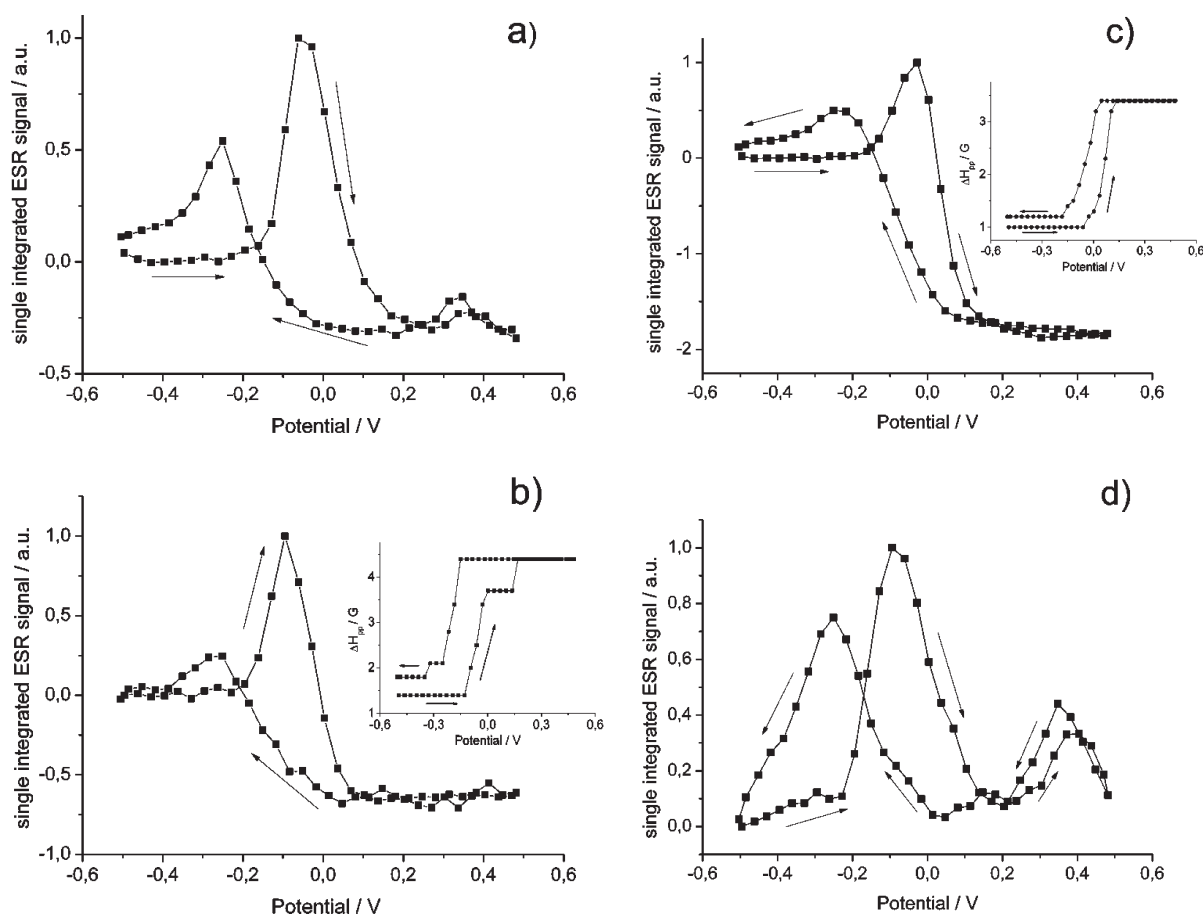


**Figure 9.** The shift of the initial bands at 306, 423, 848, and 1378 nm during the oxidation/reduction of ES.

Figure 7 gives the absorption spectra recorded in situ during the oxidation of the emeraldine salt. The band at 306 nm is attributed to the  $\pi-\pi^*$  transition of benzene rings and is characteristic for the uncharged state of ES. Under electrochemical charging, it decreases up to potentials of  $0.25$  V and increases again during the second redox peak (Figure 8). The increase of this absorbance at higher potentials points to a transformation of a part of polarons into benzene rings due to the restricted extension of the bipolarons at high potentials. Furthermore, there is a red shift of the absorption from 306 to 316 nm during the oxidation caused by the  $\pi$ -interaction of the benzene structures with the quinoid systems (Figure 9).

The bands at 423 and 848 nm appear in the spectrum of ES simultaneously at initial oxidation (Figure 7 inset and Figure 8). From potentials of  $-0.25$  V, the band at 848 nm shifts slowly to the blue region (Figure 9) and converts finally into a band at 658 nm at high oxidation level. The band at 423 nm has a red shift from potentials of  $-0.2$  V during p-doping. The potential dependence of these bands coincides with that of the ESR intensity up to potentials of  $-0.2$  V (Figure 6). The same absorption bands are observed in the spectrum of ES in *m*-cresol solution. Therefore, both bands can be associated with the formation of polarons at low oxidation level. The bands at 423 and 848 nm shift into the inverse direction, which indicates that the energy of the half filled polaron band increases obviously during the oxidation of the polymer.

The broad absorption band at 1378 nm is observed at potentials 60 mV above of those for the appearance of the bands at 423 and 848 nm. Therefore, it must be associated with the formation of other charged species. This absorption band increases up to potentials of  $0.2$  V. According to the in situ



**Figure 10.** Potential dependence of the single integrated ESR signal of EB1 (a), EB2 (b), EB3 (c), and ES (d). Insertion in (b) and (c): Potential dependence of ESR line width ( $\Delta H_{pp}$ ).

IR study of electrochemically prepared PANI and its aniline–phenosafranin copolymers, the IR bands at 1572, 1476, 1318, 1250, 1145, 1061, and 835  $\text{cm}^{-1}$  were attributed to the semi-quinoid structure of the polymer.<sup>13</sup> The potential dependence of these IR peaks does not coincide with that of the ESR signal. Therefore, the IR peaks were associated with the formation of a  $\pi$ -dimer. The  $\pi$ -dimer is formed as a face-to-face complex of two polarons interacting through their  $\pi$ -orbitals and generally characterized by two optical transitions. The second band can be hidden by the absorption of the polaron. The potential dependences of IR bands and NIR absorbance at ca. 1300 nm are in close agreement. During the second redox peak, the band at 1378 nm shifts rapidly in the blue region and transforms finally into the band at 1153 nm at a potential of 0.5 V (Figure 9).

At high electrode potentials, the absorption bands at 394, 658, and 1153 nm appear in the spectra of ES. The band at 658 nm attributed to quinoid rings points to the formation of bipolarons (protonated quinoid rings) in acidic solution at high potentials. It was confirmed by the appearance of the IR peaks at 1630 and 1375  $\text{cm}^{-1}$  at high oxidation level of PANI.<sup>13</sup> The origin of the bands at 394 and 1153 nm is not yet clear. We propose that interchain interactions between the protonated quinoid and uncharged aromatic rings occur at these potentials, leading to the formation of diamagnetic species like  $\pi$ -dimers.

**Emeraldine Base.** A summary of the potential dependencies of the ESR intensity for all polymers under study during the voltammetric scan is given in Figure 10. All polymers show ESR

signals with a small line width of ca. 2 G. The potential dependence of the single integrated ESR signal for EB1 has the second maximum with significantly lower intensity in comparison to ES. In contrary to ES and EB1, the ESR spectra of EB2 and EB3 show no ESR signal during the second redox peak. As demonstrated by FTIR and UV–vis NIR measurements, the behavior of the benzene rings dominates the polymer chains of EB1. This excess of benzene rings in EB1 and ES is a prerequisite to stabilize the trication radical formed during the second redox peak in cyclovoltammograms because of the extension of the conjugated  $\pi$ -system. In addition, changes in line width of the ESR spectra at various potentials were found (Figure 10b,c inset). The ESR line width increases during p-doping of all polymer films up to the potential of the ESR signal maximum.  $\Delta H_{pp}$  reaches a maximum at 0.2 V, where a very weak ESR signal is detected. The  $\Delta H_{pp}$  values remain unchanged in further oxidation. This behavior suggests a change of polymer structure upon doping and a decrease of the delocalization of the polarons. For ES, the ESR signal is unchanged with potential increase, and the oxidized states in the polymer are the same (Figure 10d). For emeraldine base, a strong ESR signal is detected in electrolyte solutions without any oxidation of the polymer. The difference of the ESR intensities at  $-0.5$  and  $0.5$  V increases in the row EB1–EB2–EB3. As shown by IR spectroscopy, the branching of the polymer structure increases with increasing molar weight of emeraldines. We have demonstrated earlier for electrochemically prepared PANI and the aniline–phenosafranin copolymers that the



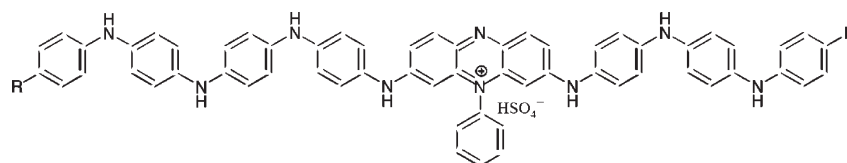


Figure 11. Structure of polyaniline containing the phenazine unit.

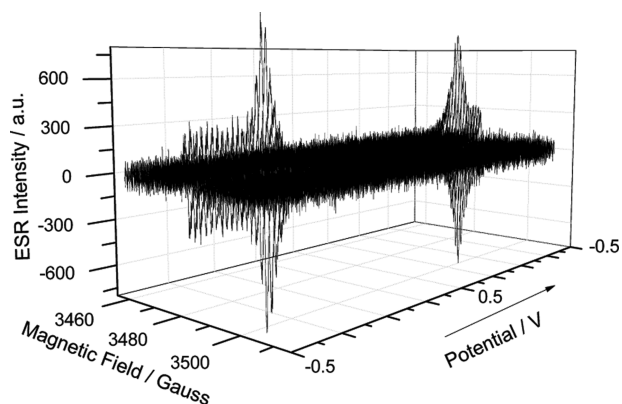


Figure 12. The ESR response of EB2 during the voltammetric scans.

phenazine-like units in the polymer structure play an important role in the stabilization of charged states in the polymer upon p-doping.<sup>13</sup> It was shown that the formation of  $\pi$ -dimers in the polymer is preferred on the linear segments of the polymer chains linked to the phenazine units as it is shown in Figure 11. Therefore, polarons are predominantly stabilized on the linear segments near the branches by phenazine in the polymer chains. EB3 as the most branched polymer structure has a maximum ESR signal in uncharged state in a row EB1–EB2–EB3.

The in situ ESR–UV–vis NIR spectroelectrochemical study of emeraldine bases upon oxidation uses EB2 as an example because the spectra of all emeraldine bases are very similar. The ESR spectrum of EB2 with a signal at  $-0.5$  V points to the presence of polarons in the uncharged state of the polymer (Figure 12) because the quinoid rings are partially protonated in acidic solution. The  $\Delta H_{pp}$  value for EB2 is 1.85 G. The ESR intensity has the first maximum at  $-0.09$  V while a second at higher potential is missing (Figure 13).

In general, the in situ UV–vis NIR spectra of emeraldine bases are similar to those of the electrochemically prepared PANI described earlier.<sup>21</sup> The absorption spectra of EB2 show some bands during its oxidation similar to those of ES (Figure 14). The absorption band at 322 nm has the same potential dependence as the band at 306 nm in the spectra of ES, but it is not shifted during the oxidation/reduction. The band at 1320 nm has a maximum at 0.2 V and appears simultaneously with the band at 448 nm at the initial stage of oxidation. The bands at 448 and 1320 nm rise at lower potentials than the ESR signal pointing to a polaron (Figure 13). The potential dependence of the absorbances at 448 and 1320 nm during oxidation of EB2 is not the same (Figure 15). In contrast to ES, the absorption band of EB2 at 448 nm shifts to the blue region upon oxidation (Figure 15 insert). This band is generally by 44 nm red-shifted in comparison to ES. Therefore, the band at 423 nm in ES and that at 448 nm in EB2 correspond to different charged species. The band at 448 nm (the second absorption is missing due to its NIR pattern) increases with charge injection before the ESR signal is

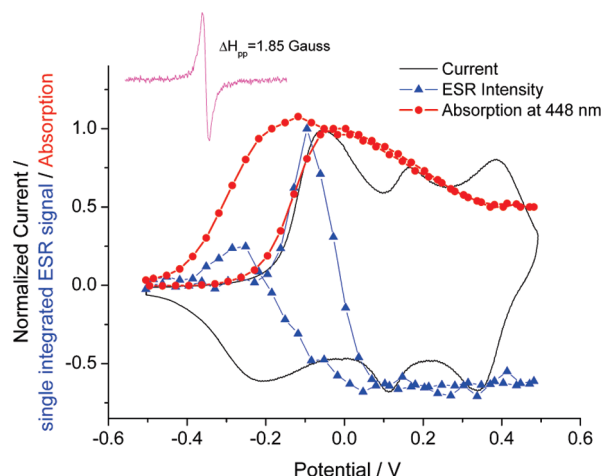


Figure 13. Potential dependence of current, single integrated ESR signal, and absorbance at 448 nm of EB2. The experimental conditions are the same as in Figure 6.

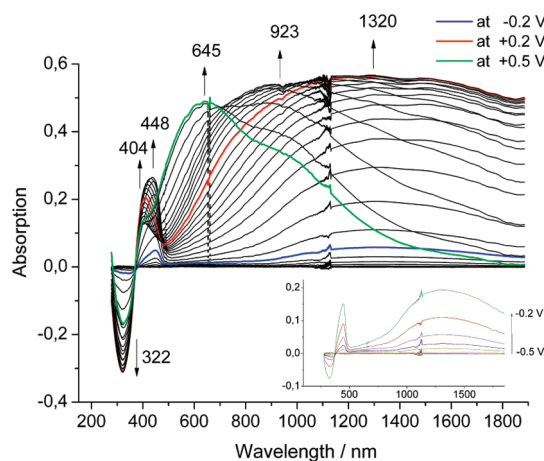
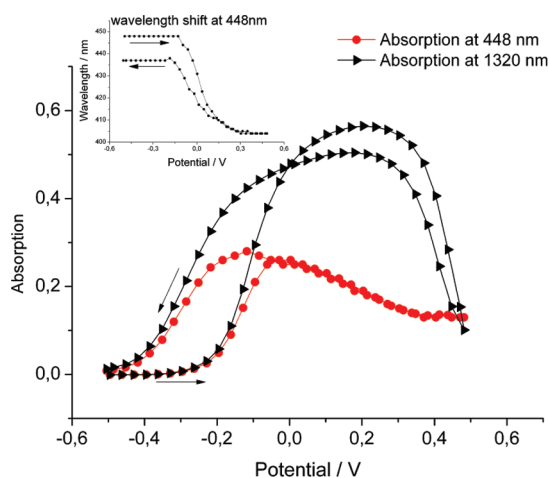


Figure 14. UV–vis NIR spectra of EB2 recorded during the forward voltammetric scan. Inset: UV–vis NIR spectra recorded in the potential region from  $-0.5$  to  $-0.2$  V.

growing and can be assigned to the formation of the spinless polaron pair (two polarons on a single chain). On the basis of the in situ FTIR measurements and the different potential dependence of the absorbances at 448 and 1320 nm, the broad band at 1320 nm was earlier attributed to the formation of  $\pi$ -dimers. This band is more intense in emeraldine base than that in ES. The band at 645 nm dominates at high oxidation level of EB2 and exists together with the bands at 404 and 923 nm.

The in situ ESR–UV–vis NIR spectroelectrochemistry of emeraldines shows a different behavior of protonated and less protonated structures of the polymer upon p-doping. The initial



**Figure 15.** Potential dependence of the absorbance at different wavelengths during oxidation/reduction of EB2. Inset: The shift of the wavelength at 448 nm.

stage of oxidation in ES prefers the formation of a polaron. The potential dependence of the ESR intensity of ES shows the second maximum during the second redox peak in the cyclovoltammogram. This second maximum is attributed to the formation of a polaronic structure interacting with bipolarons on the polymer chains (like a formal trication radical).  $\pi$ -Dimers and polaron pairs are formed at the early stage of charge injection into the emeraldine base. The branching of structure and the presence of phenazine units in the polymer stabilize the charged states in the polymer upon p-doping. EB3 with most branches in the polymer chain has a maximum ESR intensity in solutions due to the protonation of the quinoid rings of the polymer.

## CONCLUSIONS

By a combined application of different spectroscopic and spectroelectrochemical techniques, the structural details of “linear” polyaniline and their influence on the formation of charged states in the conjugated system of polyaniline has been studied in detail. By FTIR spectroscopy, it was shown that emeraldines have branches in the polymer chains and consist of small amounts of phenazine units. The IR bands at 1470, 1414, 950, 830, and 600  $\text{cm}^{-1}$  are attributed to the phenazine rings in PANI. The branching of the polymer chains increases with the increasing of the weight average molecular weight of emeraldines. The optical transitions in protonated and unprotonated emeraldine forms were investigated by UV–vis NIR spectroscopy. By comparison with the ESR spectra of emeraldines in solutions of different acidity, it was shown that the polymer consists of a polaronic structure in protic solvents and acidic solution as a consequence of the partial protonation of the polymer chains. By in situ ESR–UV–vis NIR spectroelectrochemistry, the formation of charged states in protonated and unprotonated structures of emeraldines was followed. The initial stage of oxidation in ES is preferably the polaron structure, while  $\pi$ -dimers and polaron pairs are formed by oxidation of emeraldine base. The branching structure caused by the presence of the phenazine units in the polymer chains stabilizes different charged states in the polymer upon p-doping. In conclusion, the nonideal structure of “linear” polyaniline deviating strongly from linearity has a strong influence on the type of the charged states formed upon electrochemical or proton doping.

## AUTHOR INFORMATION

### Corresponding Author

\*Tel.: +49 351 4659 660. Fax: +49 351 4659 811. E-mail: l.dunsch@ifw-dresden.de.

## ACKNOWLEDGMENT

We thank F. Ziegls, S. Schiemenz, and M. Senf (all of IFW Dresden) for technical help and BMBF for financial support to E.D.

## REFERENCES

- (1) Brédas, J. L.; Scott, J. C.; Yakushi, K.; Street, G. B. *Phys. Rev. B* **1984**, *30*, 1023.
- (2) Fesser, K.; Bishop, A. R.; Campbell, D. K. *Phys. Rev. B* **1983**, *27*, 4804.
- (3) Neudeck, A.; Petr, A.; Dunsch, L. *Synth. Met.* **1999**, *107*, 143.
- (4) Van Haare, J. A. E. H.; Havinga, E. E.; Van Dongen, J. L. J.; Janssen, R. A. J.; Cornil, J.; Brédas, J. L. *Chem.-Eur. J.* **1998**, *4*, 1509.
- (5) Petr, A.; Wei, D.; Kvarnström, C.; Ivaska, A.; Dunsch, L. *J. Phys. Chem. B* **2007**, *111*, 12395.
- (6) Van Haare, J. A. E. H.; Groenendahl, L.; Havinga, E. E.; Janssen, R. A. J.; Meijer, E. W. *Angew. Chem., Int. Ed. Engl.* **1996**, *35*, 638.
- (7) Merz, A.; Kronberger, J.; Dunsch, L.; Neudeck, A.; Petr, A.; Parkanyi, L. *Angew. Chem., Int. Ed.* **1999**, *38*, 1442.
- (8) Paasch, G.; Scheinert, S.; Petr, A.; Dunsch, L. *Russ. J. Electrochem.* **2006**, *42*, 1161.
- (9) Salaneck, W. R.; Lundström, I.; Rånby, B. *Conjugated polymers and related materials. The interconnection of chemical and electronic structure. Proceedings of the Eighty-first Nobel Symposium*; Oxford University Press: Oxford, NY, 1993.
- (10) Willstätter, R.; Moore, C. W. *Ber. Dtsch. Chem. Ges.* **1907**, *40*, 2665.
- (11) Green, A. G.; Woodhead, A. E. *Ber. Dtsch. Chem. Ges.* **1913**, *46*, 33.
- (12) Dunsch, L. Dissertation, Bergakademie Freiberg, Germany, 1973.
- (13) Kellenberger, A.; Dmitrieva, E.; Dunsch, L. *Phys. Chem. Chem. Phys.* **2011**, *13*, 3411.
- (14) Ćirić-Marjanović, G.; Trchová, M.; Stejskal, J. *J. Raman Spectrosc.* **2008**, *39*, 1375.
- (15) Trchová, M.; Šeděnková, I.; Konyushenko, E. N.; Stejskal, J.; Holler, P.; Ćirić-Marjanović, G. *J. Phys. Chem. B* **2006**, *110*, 9461.
- (16) Stejskal, J.; Sapurina, I.; Trchová, M.; Konyushenko, E. N.; Holler, P. *Polymer* **2006**, *47*, 8253.
- (17) Do Nascimento, G. M.; Silva, C. H. B.; Izumi, C. M. S.; Temperini, M. L. A. *Spectrochim. Acta, Part A* **2008**, *71*, 869.
- (18) Do Nascimento, G. M.; Silva, C. H. B.; Temperini, M. L. A. *Polym. Degrad. Stab.* **2008**, *93*, 291.
- (19) Do Nascimento, G. M.; Temperini, M. L. A. *J. Raman Spectrosc.* **2008**, *39*, 772.
- (20) Genies, E. M.; Lapkowski, M.; Penneau, J. F. *J. Electroanal. Chem.* **1988**, *249*, 97.
- (21) Dmitrieva, E.; Harima, Y.; Dunsch, L. *J. Phys. Chem. B* **2009**, *113*, 16131.
- (22) Wu, C.-G.; Yeh, Y.-R.; Chen, J.-Y.; Chiou, Y.-H. *Polymer* **2001**, *42*, 2877.
- (23) Trchová, M.; Sapurina, I.; Prokaš, J.; Stejskal, J. *Synth. Met.* **2003**, *135*, 305.
- (24) Šeděnková, I.; Trchová, M.; Blinova, N.; Stejskal, J. *Thin Solid Films* **2006**, *515*, 1640.
- (25) Ćirić-Marjanović, G.; Blinova, N.; Trchová, M.; Stejskal, J. *J. Phys. Chem. B* **2007**, *111*, 2188.
- (26) Tang, J.; Jing, X.; Wang, B.; Wang, F. *Synth. Met.* **1988**, *24*, 231.
- (27) Stammer, C.; Taurins, A. *Spectrochim. Acta* **1963**, *19*, 1625.
- (28) Socrates, G. *Infrared and Raman Characteristic Group Frequencies, Table and Charts*, 3rd ed.; John Wiley and Sons, Ltd.: Chichester, 2001; pp 107–113, 123, 157–167, 176–177, 220–222.

- (29) Li, X.-G.; Huang, M.-R.; Duan, W.; Yang, Y.-L. *Chem. Rev.* **2002**, *102*, 2925.
- (30) Chiba, K.; Ohsaka, T.; Ohnuki, Y.; Oyama, N. *J. Electroanal. Chem.* **1987**, *219*, 117.
- (31) Pouchert, C. J. *The Aldrich Library of FT-IR Spectra*, 2nd ed.; Aldrich Chemical Co.: U.S., 1985.
- (32) Trchová, M.; Šeděnková, I.; Tobolková, E.; Stejskal, J. *Polym. Degrad. Stab.* **2004**, *86*, 179.
- (33) Quillard, S.; Louarn, G.; Lefrant, S.; MacDiarmid, A. G. *Phys. Rev. B* **1994**, *50*, 12496.
- (34) Louarn, G.; Lapkowski, M.; Quillard, S.; Pron, A.; Buisson, J. P.; Lefrant, S. *J. Phys. Chem.* **1996**, *100*, 6998.
- (35) Ping, Z.; Nauer, G. E.; Neugebauer, H.; Theiner, J.; Neckel, A. *J. Chem. Soc., Faraday Trans.* **1997**, *93*, 121.
- (36) Sariciftci, N. S.; Kuzmany, H.; Neugebauer, H.; Neckel, A. *J. Chem. Phys.* **1990**, *92*, 4530.
- (37) Mitchell, M. B.; Smith, G. R.; Guillory, W. A. *J. Chem. Phys.* **1981**, *75*, 44.
- (38) Ping, Z. *J. Chem. Soc., Faraday Trans.* **1996**, *17*, 3063.
- (39) Tao, S.; Hong, B.; Kerong, Z. *Spectrochimica Acta, Part A* **2007**, *66*, 1364.
- (40) Kim, Y. H.; Foster, C.; Chiang, J.; Heeger, A. J. *Synth. Met.* **1989**, *27–29*, 285.
- (41) Stafström, S.; Brédas, J. L.; Epstein, A. J.; Woo, H. S.; Tanner, D. B.; Huang, W. S.; MacDiarmid, A. G. *Phys. Rev. Lett.* **1987**, *59*, 1464.
- (42) Xia, Y.; Wiesinger, J. M.; MacDiarmid, A. G.; Epstein, A. J. *Chem. Mater.* **1995**, *7*, 443.
- (43) Xia, Y.; MacDiarmid, A. G.; Epstein, A. J. *Macromolecules* **1995**, *27*, 7212.
- (44) Genies, E. M.; Lapkowski, M. *J. Electroanal. Chem.* **1987**, *236*, 199.